Journal of Applied Physics

Refined drift-diffusion model for the simulation of charge transport across layer interfaces in organic semiconductor devices

Cite as: J. Appl. Phys. **124**, 135501 (2018); https://doi.org/10.1063/1.5043245
Submitted: 07 June 2018 • Accepted: 31 August 2018 • Published Online: 03 October 2018

S. Altazin, C. Kirsch, E. Knapp, et al.

ARTICLES YOU MAY BE INTERESTED IN

Numerical simulation of charge transport in disordered organic semiconductor devices
Journal of Applied Physics **108**, 054504 (2010); https://doi.org/10.1063/1.3475505

Determination of charge transport activation energy and injection barrier in organic semiconductor devices
Journal of Applied Physics **122**, 115502 (2017); https://doi.org/10.1063/1.4992041

Quantitative analysis of charge transport in intrinsic and doped organic semiconductors combining steady-state and frequency-domain data
Journal of Applied Physics **124**, 105501 (2018); https://doi.org/10.1063/1.5044494

Journal of Applied Physics Special Topics Open for Submissions Learn More

AIP Publishing

© 2018 Author(s).

JOURNAL OF APPLIED PHYSICS 124, 135501 (2018)

Refined drift-diffusion model for the simulation of charge transport across layer interfaces in organic semiconductor devices

S. Altazin,[1] C. Kirsch,[2] E. Knapp,[2] A. Stous,[1] and B. Ruhstaller[1,2]
[1]*Fluxim AG, Katharina-Sulzer-Platz 2, CH-8400 Winterthur, Switzerland*
[2]*Zurich University of Applied Sciences, Institute of Computational Physics, Winterthur, Switzerland*

(Received 7 June 2018; accepted 31 August 2018; published online 3 October 2018)

We present a new approach to simulate the transport of charges across organic/organic layer interfaces in organic semiconductor devices. This approach combines the drift-diffusion formalism away from the interface with a hopping description of the charge transport in the vicinity of the interface. It has been implemented in the commercial software SETFOS allowing for fast simulations of the complete device. This new model takes into account both recombination and generation mechanisms across the interface enabling the modeling of charge-generation/recombination interfaces for the numerical simulation of tandem devices. Using this approach, it is also possible to simulate devices using 1,4,5,8,9,11-Hexaazatriphenylenehexacarbonitrile as a hole-injection layer. This particular material has a very deep HOMO level (approximately 9.5 eV), which would seemingly prevent such a layer to be used as a hole-injection material in the framework of traditional drift-diffusion models. © *2018 Author(s). All article content, except where otherwise noted, is licensed under a Creative Commons Attribution (CC BY) license (http://creativecommons.org/licenses/by/4.0/).*
https://doi.org/10.1063/1.5043245

I. INTRODUCTION

Organic light-emitting devices (OLEDs) are gaining ground as the technology for next generation devices in display and lighting applications. A crucial point for the commercialization of this new technology is to achieve stable devices with a slow degradation. One way to improve the lifetime[1] of these devices is to build OLEDs in a tandem architecture,[2] because tandem OLEDs require a lower electric current to achieve a certain luminance level compared to single-junction devices. Therefore, the device degradation is reduced. Moreover, recent record-efficiency organic photovoltaic cells (OPVs) were achieved using tandem architecture. In this application, the tandem architecture is used to stack different active materials that are sensitive to different wavelength regions of the solar spectrum. An important point for the performance of tandem devices is a good electrical connection between the different "sub-stacks." This connection is often made of an organic/organic semiconductor junction in order to minimize optical losses and in order to guarantee the integration into the manufacturing process. The goal is for this junction to act as a charge-recombination interface (CRI) (for OPVs) or as a charge-generation interface (CGI) (for OLEDs).

To our knowledge, the only attempt to perform a simulation of an organic tandem device was reported by Feiping *et al.*[3] using a previously published model from Qi *et al.*[4] to capture the physics of metal-oxide-based charge-generation units. However, their model is mainly based on the classical semiconductor theory and does not cope with the physics of organic/organic interfaces and with the hopping-transport mechanism, which is at the heart of recent developments of organic electronics.[5]

For the modeling of organic/organic interfaces, in general, several approaches have been proposed, though most of the time for single-carrier devices: Cottaar *et al.*[6] proposed a model in which the electric current at the interface can be described using an effective electric field; however, it is not clear how this approach can be generalized to the simulation of CGI or CRI interfaces involving both electrons and holes. An important point in their contribution, though, was to take into account short-range Coulomb interactions in order to reproduce Monte Carlo (MC)-simulation results of the charge transport in organic materials.

Earlier on, Ruhstaller *et al.*[7,8] proposed to modify the drift-diffusion current at the interface between two organic semiconductors by a Boltzmann factor depending on whether the drift current drives the carriers to go upward or downward in energy. Even though this approach is able to qualitatively reproduce the electrical characteristic of multilayer devices, it produces some discontinuities in the current-voltage curve when the sign of the electric field is changing at the interface of the two organic materials.

Staudigel *et al.*[9] also proposed a model to describe charge transport at the organic/organic interface in the framework of drift-diffusion simulations; however, their approach was not satisfying the thermal equilibrium[10] where the Fermi level should be constant (and continuous) across the whole device if no bias is applied. De Falco *et al.*[11] also came up with a drift-diffusion model for the simulation of bulk-heterojunction solar cells taking into account the geometry of the interface between the donor and acceptor materials; however, they considered that electrons (respectively, holes) can only be found in the donor (respectively, acceptor) materials, making this approach difficult to generalize for arbitrary combinations of materials.

Arkhipov *et al.* also studied the organic/organic interface by means of a hopping model,[12] but their approach was focused on the interface only and they were not able to simulate the whole organic device.

 © Author(s) 2018.

Here, we present a mathematical model which is able to capture the physical processes at the CGIs and CRIs described above. Our new interface model is based on the hopping-transport theory. It is coupled with the drift-diffusion formalism away from the interface, therefore, enabling fast simulations of complete devices while considering a charge-hopping model locally. This approach has been implemented in the latest version of the semiconductor device simulation software SETFOS 4.6[13] by Fluxim AG, such that users can take advantage of state-of-the-art optical, electronic, and excitonic models. This new model is available in the drift-diffusion module after introducing an interface in the layer stack. Here, we present simulation results for devices with CGIs or CRIs and we study the impact of the novel model on the simulated device performance. The results compare favorably with experimental data already published in the literature,[14,15] thus validating the model assumptions and implementation. It goes without saying that the interface-modeling approach can equally be applied to device stacks of more than two functional units (namely, multi-unit OLEDs that yield high current and luminance as well as multi-unit solar cells that yield higher power conversion efficiencies).

In Sec. II, we will describe in detail the mathematical model for the different processes occurring at the interface between two organic semiconductor materials and how to couple this interface model with the standard drift-diffusion formalism used in the bulk of these materials. In Sec. III, we will show some validation with experimental data from the literature. In Sec. IV, we will demonstrate the simulation of tandem OLED and OPV devices using the drift-diffusion formalism combined with this new model.

II. MODELING APPROACH

A. Single-carrier transport

Charge transport in organic semiconductors is locally governed by thermally assisted tunneling, often known as *hopping* between the different molecules.[16] Several ways of simulating devices made of organic semiconductors have been presented so far. Continuum models evolved from inorganic semiconductor theory and they make use of the drift-diffusion equations[17] to study materials with discrete energetic transport levels.[9,18,19] Other approaches consider the hopping transport at the molecular scale in disordered systems using kinetic Monte Carlo[20,21] or master equation (ME)[22–24] simulation. Intermediate models take into account the disordered nature of energy levels but they treat transport in a continuous way.[25–27] All approaches were able to describe the charge transport in organic semiconductor devices, but the drift-diffusion simulation is often preferred for the simulation of complex devices made of several organic layers, due to computational speed. The master equation (ME) and Monte Carlo (MC) approaches were found useful to derive effective charge-carrier mobility models[16,24] which can be used as an input for the drift-diffusion model. However, the modeling of organic/organic interfaces requires a special treatment in the drift-diffusion approach, whereas nothing special needs to be considered in a hopping-based transport model (MC or ME). A key disadvantage of ME and MC simulations is their long computation time, which is mainly related to the 3D lattice representation of the semiconductor material.

In drift-diffusion simulations, the main approach used so far for modeling the charge transport across organic/organic interfaces was to consider the continuity of the quasi-Fermi levels (for holes and electrons) across the interface.[13,28] This approach, while correct at equilibrium (no applied bias), fails to properly represent the physics at the interface far from equilibrium, when the hopping across the interface becomes a limiting factor for the transport in the device. We will show below that the quasi-Fermi level continuity condition is only valid at equilibrium or if the hopping rate is very high. Moreover, the quasi-Fermi level continuity completely neglects the possible exchange of electrons between the highest occupied molecular orbital (HOMO) on one side of the interface with the lowest unoccupied molecular orbital (LUMO) on the other side of the interface. In this section, we propose an approach to tackle this issue by coupling a hopping model in the vicinity of the interface with a drift-diffusion model away from the interface.

In a standard hopping model for electrons, the Miller-Abrahams hopping rate[23] from one site to another is given by

$$\nu\, exp\left(-q\frac{|\Delta E_{l,r}| + \Delta E_{l,r}}{2k_BT}\right) exp[-\gamma d(y, z)]. \tag{1}$$

This equation states that an electron can jump from one site to another with a rate which exponentially depends on the energy of two sites and the distance separating them. The Miller-Abrahams rate assumes that the transport is based on a phonon-assisted tunneling mechanism,[29] more details about this mechanism can be found in Ref. 30. In Eq. (1), ν represents the Miller-Abrahams pre-factor, γ the inverse tunneling distance, and $d(y, z)$ the distance between sites on opposite sides of the interface, located at coordinates y and z, respectively. $\Delta E_{l,r}$ represents the LUMO energy difference and the variation of the energy due to the electric field.

Across the interface (we assume here a single energy level for the LUMO in both organic materials, however, the model can be extended to multiple energy levels by integrating over the density of states), we have

$$\Delta E_{l,r} = LUMO_r - LUMO_l - V_r + V_l, \tag{2}$$

where the last terms, $-V_r + V_l$, accounts for the relative energy change of the of the LUMO (in eV) due to the electric field, V representing the electric potential.

In this model, we will consider, at the interface, that the electric charges can only hop from the last molecular layer on the left hand side of the interface to the first molecular layer on the right hand side of the interface (and vice versa). Therefore, we find that the total hopping rate, per second, for an electron in the LUMO on one side of the interface to the LUMO on the other side of the interface ($T_{LUMOl,LUMOr}$) can simply be expressed as the total number of available target sites multiplied by the Miller-Abrahams hopping rate:

$$T_{LUMOl,LUMOr} = \iint a_r(N_{0,r} - n_r)\nu\, exp\left(-q\frac{|\Delta E_{l,r}| + \Delta E_{l,r}}{2k_BT}\right) exp[-\gamma d(y,z)]dydz, \tag{3}$$

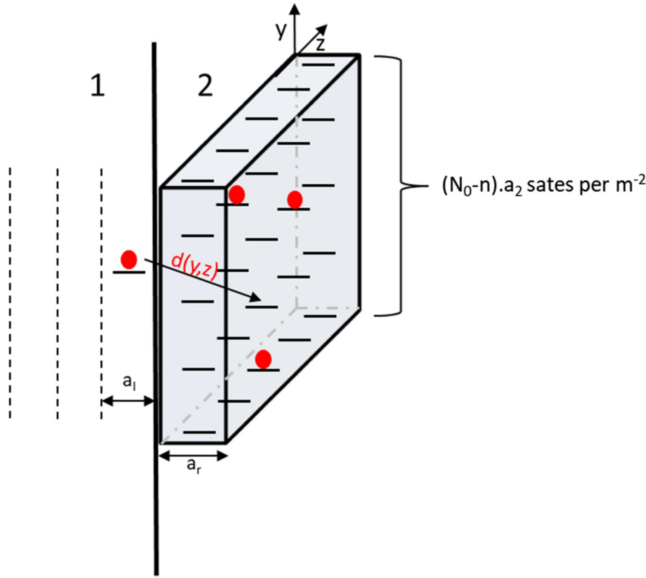

FIG. 1. Graphical representation of the number of states available in the first layer of the material on the right-hand side of the interface for a particle sitting in the last layer of material 1. The distance $d(y,z)$ between the charge and the target site has a crucial impact on the Miller-Abrahams hopping rate.

where a_r represents the inter-site distance on the right-hand side of the interface, $N_{0,r}$ the density of states on the right-hand side of the interface, and n_r the concentration of electrons on the right-hand side of the interface. Thus, the product $a_r(N_{0,2} - n_r)$ is the number of sites available (per m^2) in the first molecular layer on the right-hand side of the interface. Here, the distance $d(y,z)$, corresponds to the distance between a point in the plane before the interface at the coordinate 0, 0 and a point in the plane after the interface at coordinates y, z. This distance can be expressed as $\sqrt{\left(\frac{a_l+a_r}{2}\right)^2 + y^2 + z^2}$.

A schematic explanation of the derivation of Eq. (3) can be found in Fig. 1.

Finally, $T_{LUMOl,LUMOr}$ can be written as

$$T_{LUMOl,LUMOr} = a_r(N_{0,r} - n_r)V\, exp\left(-q\frac{|\Delta E_{l,r}| + \Delta E_{l,r}}{2k_BT}\right), \tag{4}$$

with the hopping constant V (in m^2 per second) defined as

$$V = \iint \nu\, exp[-\gamma d(y,z)]dy\,dz. \tag{5}$$

The electron flux through the interface per second per m^2 from left to right $J_{LUMOl,LUMOr}$ is given by the product of the electron number density on the left of the interface multiplied by the transfer rate $T_{LUMOl,LUMOr}$:

$$J_{LUMOl,LUMOr} = a_l n_l T_{LUMOl,LUMOr}, \tag{6}$$

where n_l represents the electron number density (per m^3) in the vicinity of the interface on the left hand side.

Similarly, the electron flux through the interface in the other direction $J_{r,l}$ can be written as

$$J_{LUMOr,LUMOl} = a_r n_r T_{LUMOr,LUMOl}, \tag{7}$$

where $T_{LUMOr,LUMOl} = a_l(N_{0,l} - n_l)V\, exp\left(-q\frac{|\Delta E_{r,l}|+\Delta E_{r,l}}{2k_BT}\right)$.

The net electron flux through the interface from left to right can finally be written as

$$J_{int,LUMO,LUMO} = J_{LUMOl,LUMOr} - J_{LUMOr,LUMOl}. \tag{8}$$

Finally, in order to take into account the charge hopping across the interface between the two organic materials in a standard discretized drift-diffusion simulator, one just needs to include the two additional equations:

$$J_{DD,left}(n_i, n_l) = J_{int,LUMO,LUMO}(n_l, n_r) = J_{DD,right}(n_r, n_{i+1}), \tag{9}$$

where $J_{DD,left}(n_i, n_l)$ (respectively, $J_{DD,right}(n_r, n_{i+1})$) represents the drift-diffusion flux on the left (respectively, right) hand side of the interface as a function of the discretized electron number density just before (respectively, after) the interface on the left (respectively, right) n_i (respectively, n_{i+1}) (see Fig. 2). The drift-diffusion flux can be approximated using the Scharfetter–Gummel scheme.[17] A graphical representation of the discretization, clarifying the notation used in the formula above, is shown in Fig. 2.

We note that in the expression of $T_{LUMOr,LUMOl}$, the Pauli exclusion principle has been assumed (an electron can only hop to a site with no electron present); however, this principle is often neglected in standard drift-diffusion simulations where the Boltzmann statistics is assumed instead of the Fermi-Dirac statistics. Indeed at low charge-carrier density, the exclusion principle does not have a big influence on the charge-carrier distribution and thus the Boltzmann statistics is a good approximation of the Fermi-Dirac statistics in this regime. The hopping rates $T_{LUMOl,LUMOr}$ (respectively, $T_{LUMOr,LUMOl}$) may be simplified in a similar manner by neglecting the occupancy of a target site with the simple approximation $N_0 - n \approx N_0$. Interestingly, using this approximation, we find the following relation from Eq. (8) at thermal equilibrium with zero net electron flux through the interface ($J_{int,LUMO,LUMO} = 0$):

$$\frac{n_r}{n_l} = \frac{N_{0,r}}{N_{0,l}} exp\left(-q\frac{\Delta E_{l,r}}{k_BT}\right). \tag{10}$$

Thus, the ratio of the electron number densities at the left

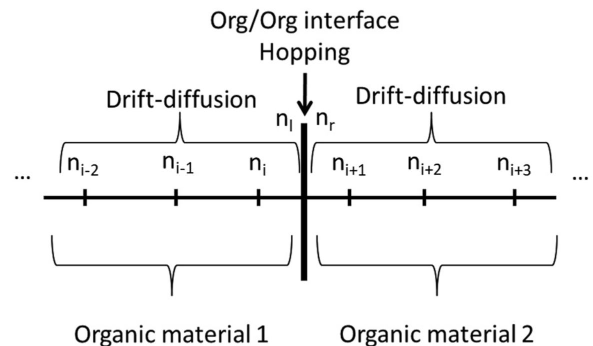

FIG. 2. Graphical representation of the discretization used in this work and implemented in the simulation software SETFOS 4.6.

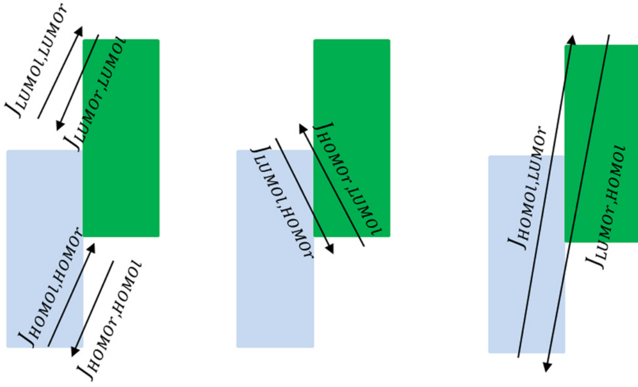

FIG. 3. Schematic representation of the different possible charge exchanges happening at the interface between two organic semiconductor materials, visualized in the molecular-energy-level diagram. The left diagram illustrates the electron exchange among HOMO levels as well as hole exchange among LUMO levels of neighboring materials. The middle diagram represents the charge generation and recombination across the layer interface, whereas the right diagram again visualizes generation and recombination across a larger energy gap.

and right sides of the interface is determined by the jump in the LUMO energy across the interface and the device temperature if the occupancy of target sites is neglected. This means that we find the Fermi-level continuity across the interface in this approximation. A similar result can be obtained for a non-zero current assuming that the parameter ν of the Miller-Abrahams hopping rate is very high (i.e., the charges across the interface tend to reach their equilibrium very fast). This means that the developed model can be seen as an extension of the more standard quasi-Fermi level continuity for situations out of equilibrium.

B. Bipolar devices

The approach presented for electrons in the first part can be derived in a similar way for holes. Moreover, it can be extended in order to consider electrons hopping from the LUMO on one side of the interface to the HOMO on the other side of the interface, which corresponds to interface recombination. Also, in order to satisfy the detailed-balance principle,[31] the reverse process has to be considered: where electrons from the HOMO on one side of the interface jump in the LUMO on the other side, which corresponds to interface generation. This latter effect, which is not obvious at first sight, is of primary importance to simulate a hole-injecting layer with a very deep LUMO level (approximately 5.5 eV) such as 1,4,5,8,9,11-Hexaazatriphenylenehexacarbonitrile (HAT-CN)[32] used in OLEDs. An example of an OLED making use of a HAT-CN injection layer is shown in the supplementary material.

A schematic representation of all the possible charge exchanges happening across the interface is summarized in Fig. 3.

Using a similar concept as in Sec. II A, the electron hopping flux from the LUMO on the left to the HOMO on the right ($J_{LUMOl,HOMOr}$) can be written as

$$J_{LUMOl,HOMOr} = a_l n_l T_{LUMOl,HOMOr}, \tag{11}$$

with the hopping rate defined as

$$T_{LUMOl,HOMOr} = a_r p_r V \exp\left(-q\frac{|\Delta E_{LUMOl,HOMOr}| + \Delta E_{LUMOl,HOMOr}}{2k_B T}\right). \tag{12}$$

In the reverse process, electrons hop from the HOMO on the right-hand side to the LUMO on the left-hand side with a flux given by

$$J_{HOMO2,LUMO1} = a_r(N_{0,r} - p_r)T_{HOMOr,LUMOl}, \tag{13}$$

where the rate is defined as

$$T_{HOMOr,LUMOl} = a_l(N_{0,l} - n_l)V \exp\left(-q\frac{|\Delta E_{HOMOr,LUMOl}| + \Delta E_{HOMOr,LUMOl}}{2k_B T}\right). \tag{14}$$

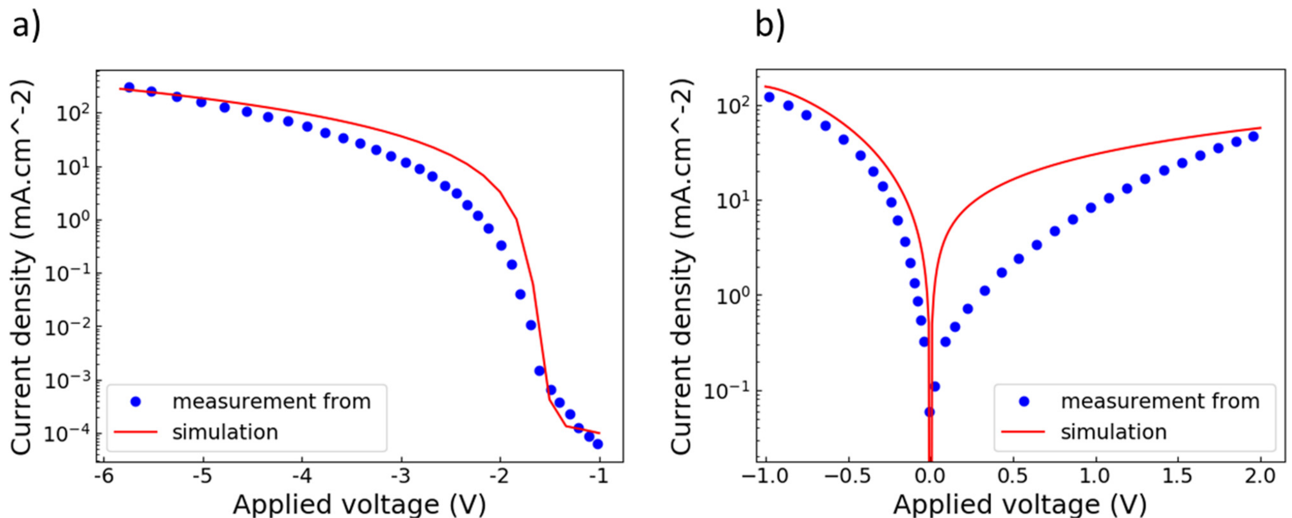

FIG. 4. Comparison of experimental current-voltage characterization from the literature and simulations using SETFOS of bilayer devices exhibiting charge-carrier generation properties. (a) refers to Sakanoue *et al.*[14] and their experiment with F16CuPc/m-MTDATA bilayers, whereas (b) refers to Opitz *et al.*[15] and their experiment with H16CuPc/F16CuPc bilayers. See table S1 and table S2 in supplementary material for a list of the material parameters.

Therefore, in order to include these new hopping fluxes within the drift-diffusion formalism, similar to Eq. (9), one has to solve the following equations:

$$J_{DD,left}(n_i, n_l) = J_{int,LUMO,LUMO}(n_l, n_r) + J_{LUMOl,HOMOr}(n_l, p_r) - J_{HOMOr,LUMOl}(n_l, p_r), \quad (15)$$

$$J_{DD,right}(n_r, n_{i+1}) = J_{int,LUMO,LUMO}(n_l, n_r) + J_{HOMOl,LUMOr}(p_l, n_r) - J_{LUMOr,HOMOl}(p_l, n_r). \quad (16)$$

In the above equations, each term depends on two charge carrier number densities of neighboring sites according to the discretization scheme of Fig. 2. Two similar equations can be derived for the continuity of the hole current.

While we have introduced four new unknowns for the hole and electron number densities at the interface (n_l, n_r, p_l, p_r), indeed in the standard approach (without this new organic/organic interface), no charge density point would coincide with the interface between the two organic materials. These unknowns are related via the four new equations introduced here. These four unknowns can be determined by solving the four new equations that have been introduced [Eqs. (15) and (16) and similar ones for the hole-current continuity]. This new model for the simulation of organic/organic interfaces has been incorporated in the commercial semiconductor device simulation software SETFOS.[13]

III. COMPARISON WITH EXPERIMENTAL RESULTS

In order to validate the modeling approach introduced in Sec. II, measurements reported in the literature have been qualitatively compared with SETFOS simulations. In order not to introduce too many unknown parameters and as a proof of concept, only simple device stacks representing

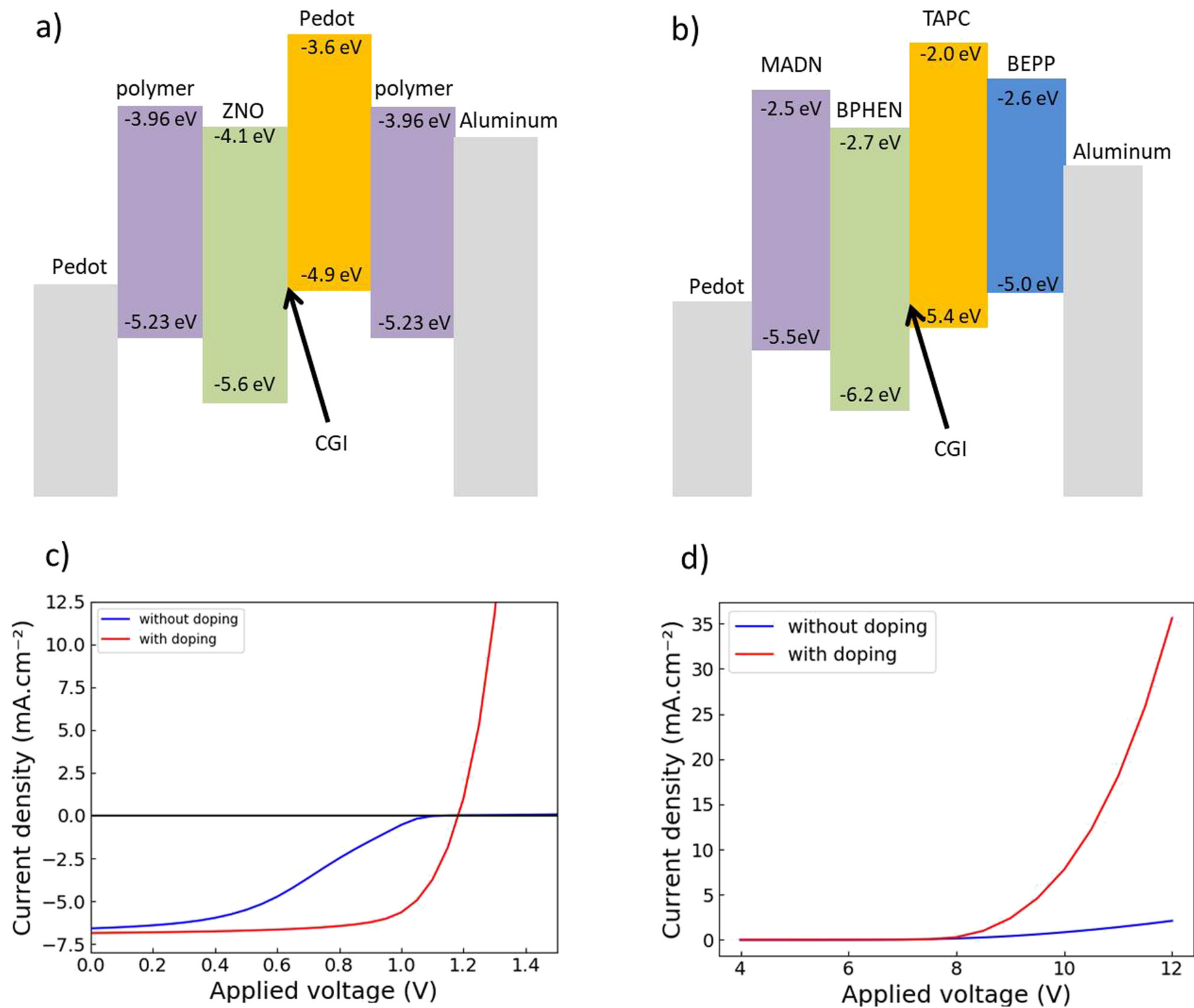

FIG. 5. Energy diagram for the simulated tandem OPV composed of two sub-cells with identical active-layer material ("polymer") (a) and of the tandem OLED inspired by the publication of Springer *et al.* (b). Simulated IV curve of the corresponding device with or without doping the layers surrounding the CRI and CGI, respectively, (c) and (d). We also show the IV curve of a single cell device in (c) and (d) (green) for comparison. See table S3 and table S4 in supplementary material for a list of the material parameters.

CGIs for tandem OLEDs or for hole injection have been simulated. The first one is from Sakanoue *et al.*[14] In this publication, the authors fabricated a bilayer device made of F16CuPc (LUMO = 4.9 eV, HOMO = 6.3 eV) and $C_{57}H_{48}N_4$ (m-MTDATA) (LUMO 1.85 eV, HOMO 5.0 eV), the former being a good electron-conducting material and the latter being a common hole-transport material. Using this combination of materials and aluminum electrodes, the authors noticed an unusually high reverse current which cannot be attributed to electrons and holes injected from the electrodes. They attributed this current to the generation of charge carriers across the interface—indeed the small energy difference between the LUMO level of F16CuPc and the HOMO of m-MTDATA (0.1 eV) allows electrons from the HOMO of m-MTDATA to hop into the LUMO of F16CuPc at room temperature. Using SETFOS, we were able to nicely reproduce this behavior (see Fig. 4). There are several reasons why the current increases when a voltage is applied: first, charges are injected in the device and due to the drift and the diffusion, they can move away from the injecting interface. Then at the organic-organic interface, the current will increase because more charge carriers will be present on one side of the interface and less on the other side, therefore favoring the transfer of charges across the interface.

Similar findings were obtained with the second example from the literature published by Opitz *et al.*[15] where a bilayer PEDOT:PSS/H16CuPc/F16CuPc/LiF/Al device was characterized. We can also notice that the forward current (injected at the electrodes) is less than the reverse current (generated at the interface). The same observation was made by Opitz *et al.*[15] when interpreting the IV characteristic of their device. For the simulation, we have assumed injection-barrier heights of 0.3 eV and that the HOMO of the H16CuPc was lying only 0.2 eV below the LUMO. In the original publication, the authors reported an interlayer HOMO-LUMO energy gap of 1.2 eV; however, this value seems too large to allow electrons from the F16CuPc to hop into the H16CuPc at room temperature, unless some interfacial effects such as dipoles or band bending can reduce this energy difference. At this stage, we did not intend to introduce additional parameters in the simulation and, therefore, neglected these two effects such that the simulation result in Fig. 4 agrees with experimental data only qualitatively. Nevertheless, we will see in

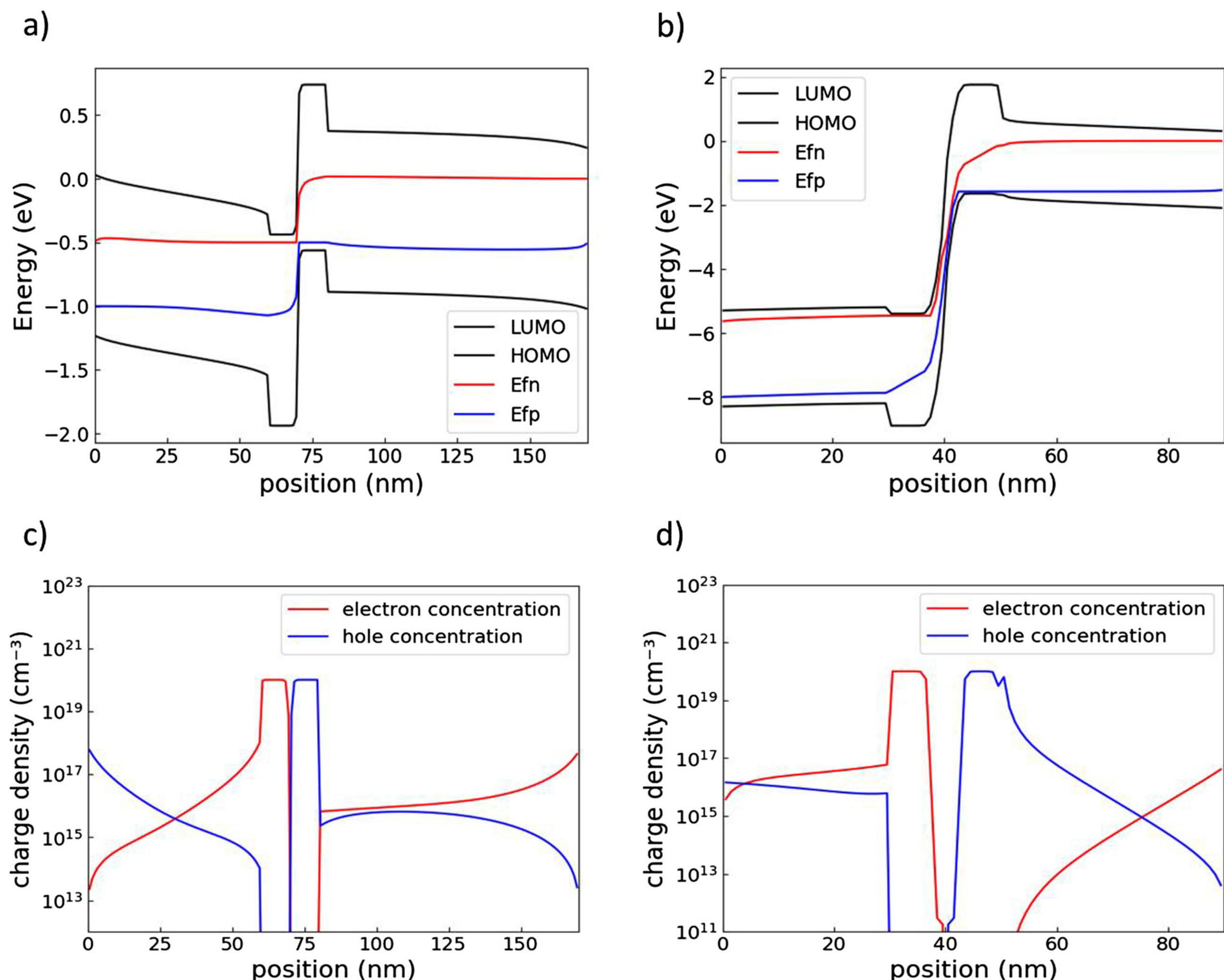

FIG. 6. Band diagram of the tandem OPV (a) at Maximum Power Point (MPP) (1 V applied) and corresponding charge-carrier densities (c). Band diagram of the tandem OLED (b) at 8 V (corresponding to the turn-on voltage of the device) and corresponding charge-carrier densities (d). The dotted lines represent the interfaces between the different layers. The n- and p-doped layers next to the CRI and CGI are 10 nm thin in these simulation examples.

Sec. IV that considering charge doping of the layers surrounding the CGI is crucial for the quantitative simulation of tandem devices. We also notice that the simulated forward (injected) current [see Fig. 4(b)] does not match properly with the experimental results (from Opitz *et al.*). This fit could be improved by introducing field-dependent motilities. However, we did not want to complicate the simulation since the main observations can already be reproduced qualitatively.

IV. SIMULATION OF TANDEM DEVICES

In this section, we demonstrate that our new interface model can be used to simulate tandem devices that contain CGI or CRI bilayers. Both a homo-tandem OPV device, with the same active materials in both sub-cells, and a tandem OLED (Organic Light Emitting Diode) have been simulated (inspired from Springer *et al.*[33]; see Fig. 5). Concerning the tandem OPV (Organic Photovoltaic Device), the high open-circuit voltage can be attributed to the indirect serial connection of the two sub-cells. It is noteworthy that this high open-circuit voltage (see Fig. 5), which is higher than the built-in voltage induced by the electrode work-function difference, cannot normally be achieved in standard drift-diffusion simulations without using an additional interface model as described in Sec. II of this contribution.

It is also important to notice that the CGI of the tandem OLED is located between two materials with a rather large HOMO-LUMO difference (more than 2 eV for the OLED case and more than 0.8 eV for the OPV case). This is necessary in order to ensure the electron (respectively, hole) injection into the adjacent layers. Even though the charge generation appears impossible at first sight (due to the high HOMO-LUMO difference), it actually takes place due to the high potential drop (i.e., strong electric field) across the interface, therefore, decreasing the effective energy difference between the HOMO and the LUMO [see Eq. (2)]. This last point can be observed in Figs. 6(a) and 6(b), where we can notice the strong bending of the HOMO and the LUMO at the CRI and CGI. This potential drop is achieved by using heavily doped layers surrounding the CGI: the n- and p-doping across the interface leads to a local PN junction with a strong electric field in the space-charge region (i.e., near the interface). In the simulation examples shown in Figs. 5 and 6, charge-doping levels on the order of $10^{20}\,\mathrm{cm}^{-3}$ are used. Without the charge dopant, the charge generation across the interface would not be efficient enough and would, therefore, limit the electric current flowing through the device. A simulation example for a tandem solar cell without electrical doping of the charge-generation unit is shown in Fig. 5(c). We can notice the strong S shape appearing and the low current flowing through the device if the applied voltage is above the open-circuit voltage. Similar results are found in the OLED case where the current across the device is strongly reduced when removing the CGI charge dopants in the simulation [see Fig. 5(d)].

Also, in these simulations, the hopping parameter V was chosen such that the generation/recombination across the interface was not limiting the current through the device, a value of $5 \cdot 10^{-3}\,\mathrm{m}^2\,\mathrm{s}^{-1}$ was chosen for the OLED case and a value of $5 \cdot 10^{-7}\,\mathrm{m}^2\,\mathrm{s}^{-1}$ was chosen for the OPV case. Therefore, the choice of this value was not yet motivated by a physical consideration, either *ab initio* modeling using the Marcus theory[34] or suitable experiments, to be defined, could help for the calculation of this rate.

The charge-carrier profiles are shown in Fig. 6, where we can notice the good injection properties from the doped layers (surrounding the CRI and CGI) in the neighboring active layers, moreover, the hole and electron concentrations remain approximately constant in these layers due to the strong electrical doping.

V. CONCLUSIONS

In this contribution, a new and refined model for the charge transport across organic semiconductor interfaces was presented. This model is based on the hopping theory, and it is coupled to the standard drift-diffusion model away from the interface for a complete device simulation. It is found that this model can be seen as an extension and generalization of the more standard quasi-Fermi level continuity found in most drift-diffusion solvers available today. Moreover, by taking into account the possible transfers of electrons from the HOMO to the LUMO across the interface, it has been shown that this model can be used to simulate CGIs and CRIs and, therefore, tackle tandem and multi-unit devices (both OLEDs and OPVs). Thereby we have demonstrated that the standard hopping theory coupled with a standard drift-diffusion transport equation is able to master the complexity of charge transport across organic/organic interfaces. The modeling of organic/organic interfaces as presented in this contribution could be further refined by introducing an effective field at the interface as in Ref. 6 but also by introducing a local density of states in the vicinity of the interface as suggested in Ref. 35. Further investigations should be directed toward the choice of the value for the hopping rate pre-factor (V). Also, the presence of interface charges should be investigated further by means of both simulations and characterization techniques, as it can have a strong impact on the local electric field,[36] therefore impacting the hopping rate. Finally, this model could also be generalized for 2D or 3D drift-diffusion device simulators.

SUPPLEMENTARY MATERIAL

See supplementary material for the simulation of OLEDs using HAT-CN as a hole-injection material.

ACKNOWLEDGMENTS

We acknowledge financial support from the Swiss National Science Foundation (SNSF; Project No. 151563) within the CARDYN Project.

[1] D. Y. Kondakov, J. R. Sandifer, C. W. Tang, and R. H. Young, J. Appl. Phys. **93**, 1108 (2003).
[2] J. Kido, M. Kimura, and K. Nagai, Science **267**, 1332 (1995).
[3] F. Lu, Y. Peng, and Y. Xing, J. Semicond. **35**, 44005 (2014).
[4] X. Qi and S. R. Forrest, J. Appl. Phys. **110** 124516 (2011).

[5]K. Walzer, B. Maennig, M. Pfeiffer, and K. Leo, Chem. Rev. **107**, 1233 (2007).
[6]J. Cottaar, R. Coehoorn, and P. A. Bobbert, Org. Electron. **13**, 667 (2012).
[7]B. Ruhstaller, S. A. Carter, S. Barth, H. Riel, W. Riess, and J. C. Scott, J. Appl. Phys. **89**, 4575 (2001).
[8]B. Ruhstaller, E. Knapp, B. Perucco, N. Reinke, D. Rezzonico, and F. Müller, in *Optoelectronic Devices and Properties* (InTech, 2011), pp. 433–458.
[9]J. Staudigel, M. Stößel, F. Steuber, and J. Simmerer, J. Appl. Phys. **86**, 3895 (1999).
[10]W. Tress, *Organic Solar Cells* (Springer International Publishing, Cham, 2014).
[11]C. de Falco, M. Porro, R. Sacco, and M. Verri, Comput. Methods Appl. Mech. Eng. **102**, 245–246 (2012).
[12]V. I. Arkhipov, E. V. Emelianova, and H. Bässler, J. Appl. Phys. **90**, 2352 (2001).
[13]SETFOS 4.6 user manual by Fluxim AG (2018).
[14]T. Sakanoue, T. Irie, and C. Adachi, J. Appl. Phys. **105** 114502 (2009).
[15]A. Opitz, B. Ecker, J. Wagner, A. Hinderhofer, F. Schreiber, J. Manara, J. Pflaum, and W. Brütting, Org. Electron. Phys. Mater. Appl. **10**, 1259 (2009).
[16]R. Coehoorn, W. F. Pasveer, P. A. Bobbert, and M. A. J. Michels, Phys. Rev. B **72**, 155206 (2005).
[17]S. Selberherr, *Analysis and Simulation of Semiconductor Devices* (Springer-Verlag, 1984).
[18]E. Knapp and B. Ruhstaller, J. Appl. Phys. **112** 024519 (2012).
[19]S. Altazin, R. Clerc, R. Gwoziecki, J. M. Verilhac, D. Boudinet, G. Pananakakis, G. Ghibaudo, I. Chartier, and R. Coppard, J. Appl. Phys. **115**, 1 (2014).
[20]J. J. M. van der Holst, F. W. A. van Oost, R. Coehoorn, and P. A. Bobbert, Phys. Rev. B **83**, 85206 (2011).
[21]H. Houili, E. Tutiš, H. Lütjens, M. N. Bussac, and L. Zuppiroli, Comput. Phys. Commun. **156**, 108 (2003).
[22]M. Z. Szymanski, I. Kulszewicz-Bajer, J. Faure-Vincent, and D. Djurado, Phys. Rev. B Condens. Matter Mater. Phys. **85**, 1 (2012).
[23]C. Jungemann, J. Comput. Electron. **14**, 37 (2015).
[24]W. F. Pasveer, J. Cottaar, C. Tanase, R. Coehoorn, P. A. Bobbert, P. W. M. Blom, M. De Leeuw, and M. A. J. Michels, Phys. Rev. Lett. **94**, 1 (2005).
[25]S. L. M. van Mensfoort and R. Coehoorn, Phys. Rev. B **78**, 85207 (2008).
[26]E. Knapp and B. Ruhstaller, Opt. Quantum Electron. **42**, 667 (2011).
[27]Y. Roichman and N. Tessler, Appl. Phys. Lett. **80**, 1948 (2002).
[28]K. Hess, M. Grupen, K. Hess, and G. H. Song, in *Proceedings of Fourth International Conference on Simulation of Semiconductor Devices and Processes* (Springer-Link, 1991), Vol. 4, pp. 303.
[29]N. Tessler, Y. Preezant, N. Rappaport, and Y. Roichman, Adv. Mater. **21**, 2741–2761 (2009).
[30]A. Miller and E. Abrahams, Phys. Rev. **120**, 745 (1960).
[31]W. Zhou, C. Zimmermann, and C. Jungemann, IEEE Trans. Electron Devices **63**, 4919 (2016).
[32]L. S. Liao and K. P. Klubek, Appl. Phys. Lett. **92**, 223311 (2008).
[33]R. Springer, B. Y. Kang, R. Lampande, D. H. Ahn, S. Lenk, S. Reineke, and J. H. Kwon, Opt. Express **24**, 28131 (2016).
[34]G. R. Hutchison, M. A. Ratner, and T. J. Marks, J. Am. Chem. Soc. **127**, 16866 (2005).
[35]M. Oehzelt, N. Koch, and G. Heimel, Nat. Commun. **5**, 1 (2014).
[36]S. Altazin, S. Züfle, E. Knapp, C. Kirsch, T. D. Schmidt, L. Jäger, Y. Noguchi, W. Brütting, and B. Ruhstaller, Org. Electron. **39**, 244 (2016).